Supplementary Information

Title: **All-dielectric bilayer complementary metasurfaces supporting quasi-bound states in the continuum induced by intrinsically broken out-of-plane symmetry**

Kwang-Hyon Kim
Institute of Physics, State Academy of Sciences, Unjong District, Pyongyang, Democratic People's Republic of Korea
Corresponding Author E-mail: kwang-h.kim@star-co.net.kp (Kwang-Hyon Kim)

S1. Multipole decomposition

In order to disclose the multipolar nature of the quasi-BIC, we perform the multipole decomposition for the resonant mode shown in Figure 1. Figure S1a presents the transmission and reflection spectra as shown in Figure 1c and the corresponding results of multipole decomposition in Figure S1b.

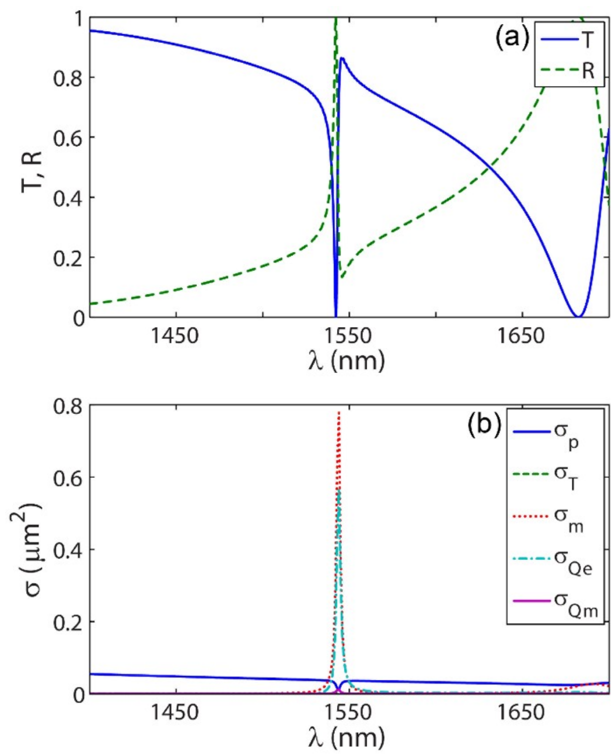

Figure S1. Transmission T and reflection spectra R (a) and the corresponding multipole decomposition result (b). The structural and material parameters are the same as in Figure 1c-e.

The Cartesian electric dipole p, toroidal dipole T, magnetic dipole m, electric quadrupole $\hat{Q}$, and magnetic quadrupole moments $\hat{M}$ are described as follows [S1]:

$$
\begin{cases}
p = \int P d^3 r, \\
T = \frac{k^2}{10}\int [(r \cdot P)r - 2r^2 P] d^3 r, \\
m = -\frac{i\omega}{2}\int (r \times P) d^3 r, \\
\hat{Q} = \int [3(r \otimes P + P \otimes r) - 2(r \cdot P)\hat{U}] d^3 r, \\
\hat{M} = \frac{\omega}{3i}\int [(r \times P) \otimes r + r \otimes (r \times P)] d^3 r,
\end{cases}
$$

where $P = \varepsilon_0(n^2 - 1)E$ is the induced polarization, E and ω are the electric field and angular frequency of light, n is the refractive index, ε_0 is the permittivity of vacuum, $\hat{U}$ is the 3×3 unity tensor, respectively. In the long wavelength approximation ($kr \ll 1$), the total scattering cross-section can be approximately determined by [S1]

$$
\sigma_{sca} \approx \frac{k^4|p + T|^2}{6\pi\varepsilon_0^2|E_0|^2} + \frac{k^4\mu_0|m|^2}{6\pi\varepsilon_0|E_0|^2} + \frac{k^6\sum|\hat{Q}|^2}{720\pi\varepsilon_0^2|E_0|^2} + \frac{k^6\mu_0\sum|\hat{M}|^2}{80\pi\varepsilon_0|E_0|^2},
$$

where μ_0 is the permeability of vacuum, E_0 is the electric field of incident light, and $k = \omega/c$, respectively. In Figure S1b, we have shown the individual contributions f each multipoles to the total scattering. As shown in the figure, the magnetic dipole and electric quadrupole simultaneously contribute to the narrow resonant peak at 1542 nm, which is consistent with the results for the local field distributions shown in Figure 1d,e.

S2. Quasi-BIC originating from TE guiding mode

For unperturbed slab structure, both TM and TE guiding modes play the roles of BIC. From the result shown in Figure 4b, the period of the metasurface is taken to be $p_x = p_y = 560$ nm, for which TE -originated BIC appears at around 1550 nm. The thickness of silicon layer and the diameter of silica disk are $h = 200$ nm and $D = 200$ nm, respectively. Here, we present the evolution of quasi-BIC with respect to the asymmetry parameter δ. Figure S2a,b presents the transmission and reflection spectra as the functions of δ, and the corresponding resonant wavelength λ_0 and Q-factor Q are shown in Figure S2c,d, respectively. As can be seen in Figure S2a,b, the transmission and reflection spectra exhibit the typical behavior as quasi-BIC for the change of asymmetry parameter δ. The resonant wavelength λ_0 slightly decreases from 1544 nm to 1509 nm for the increase of δ from 20 nm to 100 nm (Figure S2c). In the meantime, Q-factor drastically decreases from 1413 to 96.9 for the same variation of δ (Figure S2d). The field distributions shown in Figure S2e,f clearly reveal the nature of the quasi-BIC as TE mode with the non-zero components of E_x, H_y, and H_z, respectively.

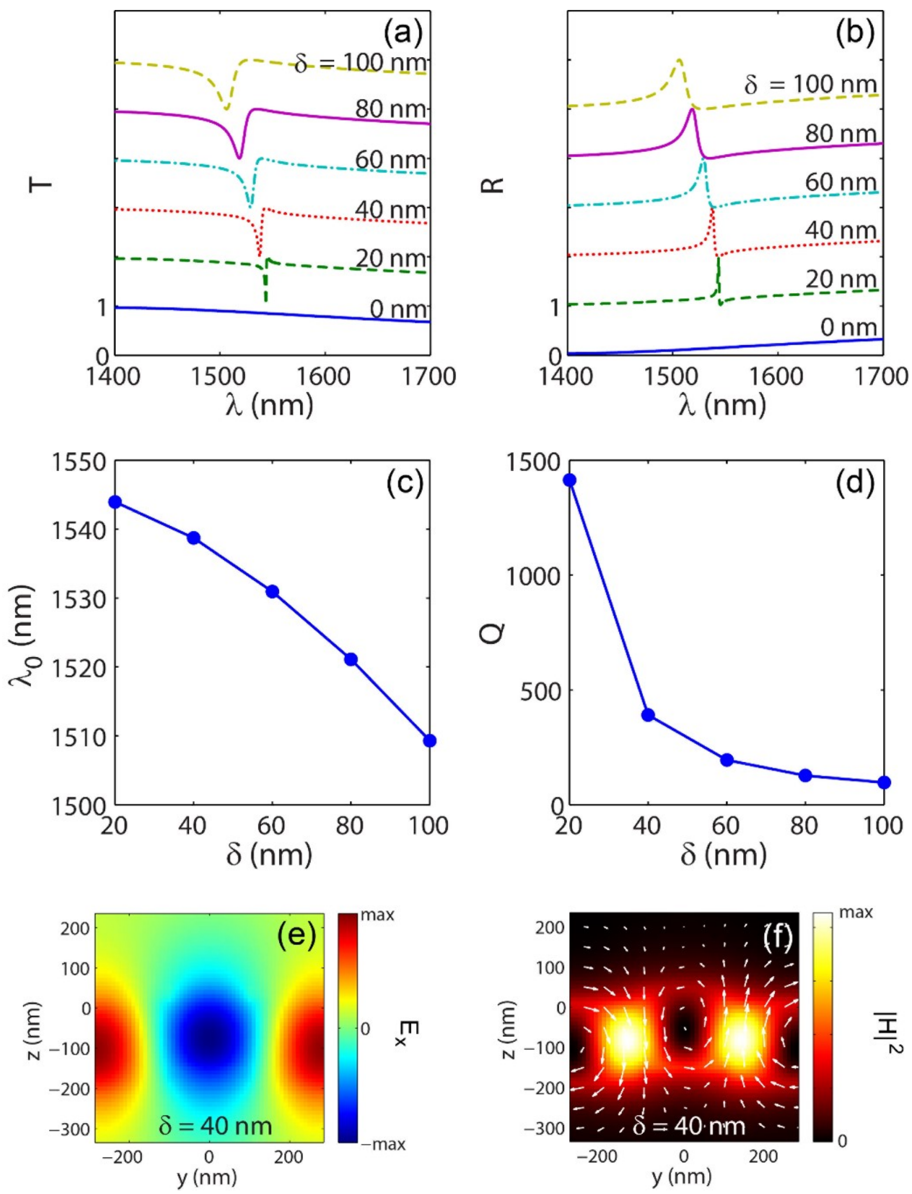

Figure S2. Transmission (a) and reflection spectra (b) as the functions of asymmetry parameter δ. The corresponding resonant wavelength λ_0 and Q-factor Q are shown in (c) and (d), respectively. The transverse electric field component E_x (e) and the squared magnetic field $|H|^2$ (f) are shown in yz-plane at the resonant wavelength 1539 nm for $\delta = 40$ nm. The periods along x- and y-directions are $p_x = p_y = 560$ nm, the thickness of silicon layer is $h = 200$ nm, and the diameter of silica disk is $D = 200$ nm, respectively.

S3. Transmission and reflection spectra as the functions of structural parameters

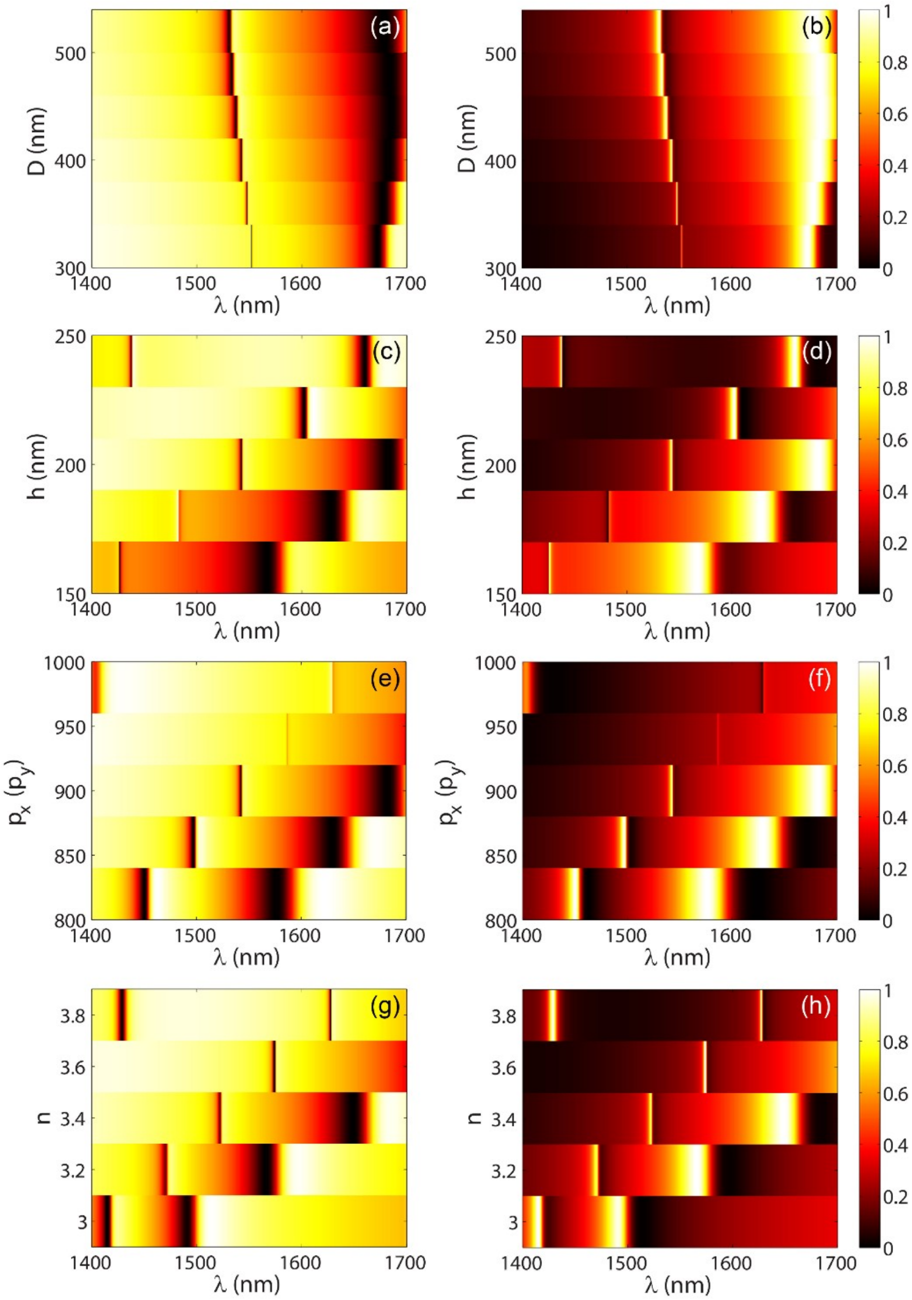

Figure S3. Transmission T and reflection spectra R as the functions of the structural parameters: the diameter D of silica nanodisks (a,b), the thickness h of silicon layer (c,d), the periods p_x and p_y of the metasurface (e,f), and the refractive index n of the high-index layer (g,h), respectively. Transmission spectra are shown in (a), (c), (e), and (g) , while the reflection ones are presented in (b), (d), (f), and (h), respectively. The other structural and material parameters are the same as in Figure 1.

S4. Polarization-dependent quasi-BIC

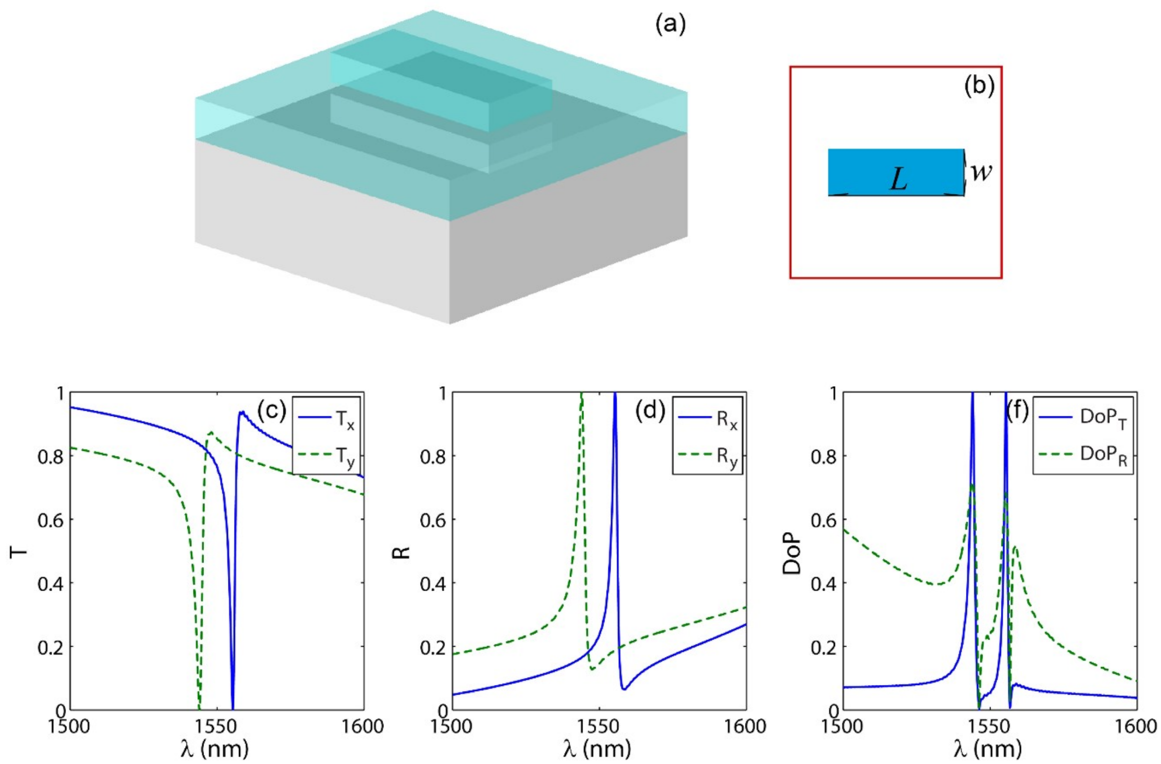

Figure S4. Unit cell structure (a,b) of a dielectric complementary bilayer polarization-dependent metasurface. In (b), $L = 560$ nm and $w = 240$ nm, respectively. The height of silica nanobar is 140 nm and the thickness of silicon layer is 200 nm, respectively. In (c) and (d), the transmission T and reflection spectra R are shown for the incident lights which are linearly polarized along x- and y-directions, which are parallel to the long and short axes of silica nanobars, respectively. In (f), the degrees of polarization defined as $DoP = \left||E_x|^2 - |E_y|^2\right|/\left(|E_x|^2 + |E_y|^2\right)$ are shown for both transmitted and reflected lights.

If we take the complementary bilayer metasurface with unit cells composed of nanobars with different lengths along the orthogonal in-plane directions instead of nanodisks, we can obtain strongly resonant linearly polarized optical response, as shown in Figure S4. The unit cell structure is shown in Figure S4a,b, where $L = 560$ nm and $w = 240$ nm (Figure S4b), the height of silica nanobar is 140 nm and the thickness of silicon layer is 200 nm, respectively. As shown in Figure S4c-f, such a metasurface exhibits strongly polarization-dependent response with high Q-factors of 682 and 881 at the wavelengths of 1544.6 nm and 1555.4 nm, at which the transmitted and reflected lights are linearly with the degree of polarization (DoP) of almost unity, respectively. Here, the degree of polarization DoP is defined as the ratio of intensity of linearly polarized component to the total intensity:

$DoP = \left||E_x|^2 - |E_y|^2\right| / \left(|E_x|^2 + |E_y|^2\right)$, where E_x and E_y are the x- and y-components of the electric field of transmitted and reflected lights, respectively.

S5. Dependence of circular dichroic optical response on the structural parameters

In Figures S5-S7, we present the structural parameter dependence of chiroptical response of the metasurface shown in Figure 6. The metasurface structure is the same as in Figure 6 and the definitions for the structural parameters a, b, and w can be found in the inset of Figure 6a.

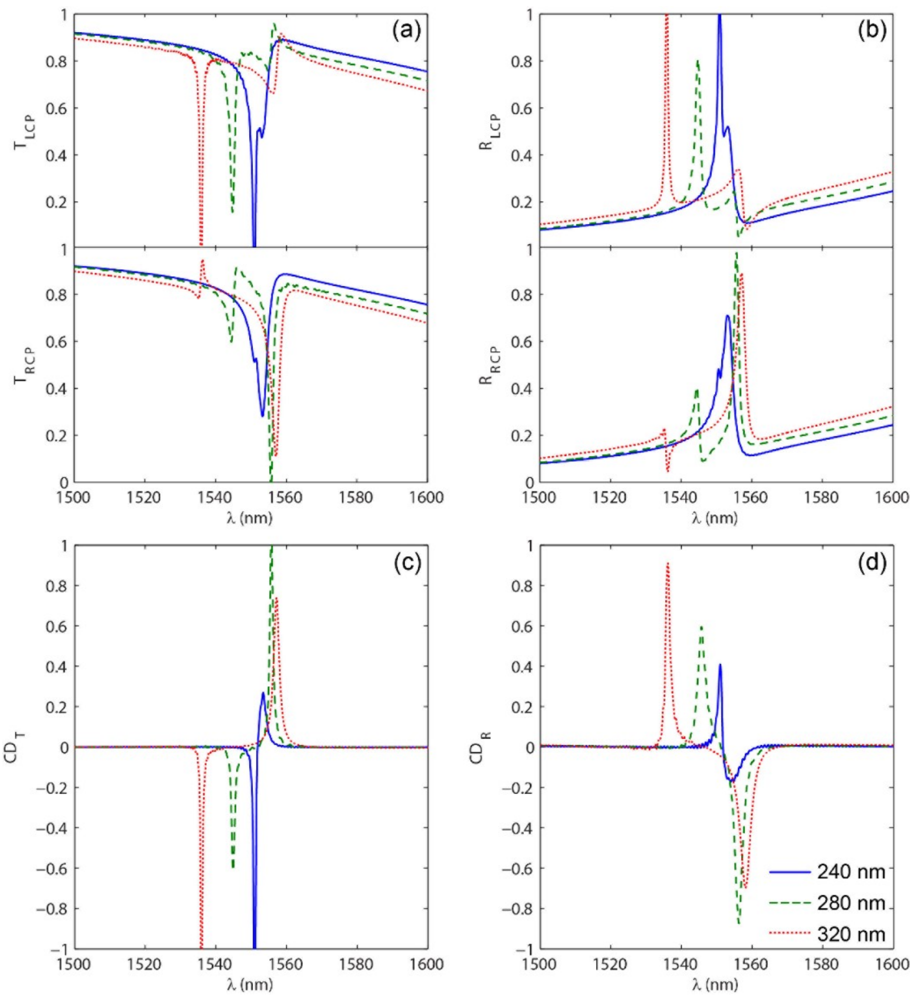

Figure S5. Transmission T (a) and reflection spectra R (b) for LCP and RCP incidences and different values of a, the definition of which can be found in the inset of Figure 6a. The resultant circular dichroism for transmitted CD_T and reflected lights CD_R are shown in (c) and (d), respectively. Blue solid lines, green dashed, and red dotted ones represent the results for $a = 240$ nm, 280 nm, and 320 nm, respectively. The other structural and material parameters are the same as in Figure 6.

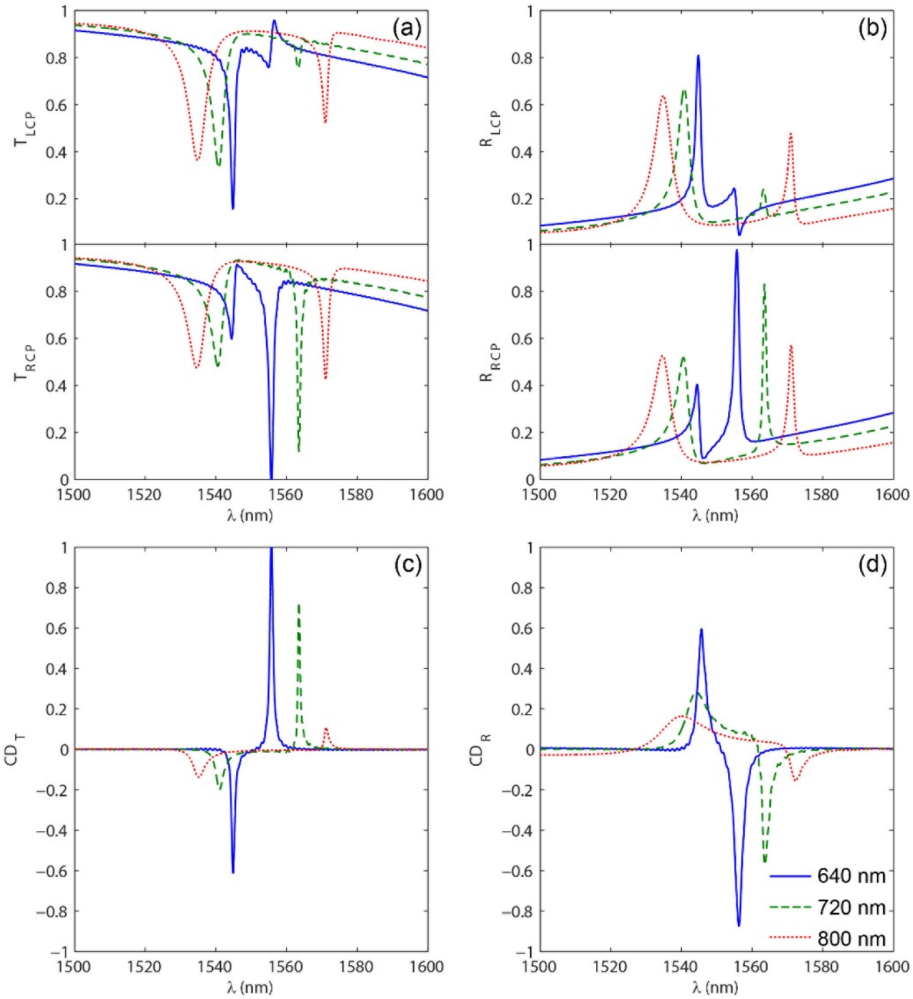

Figure S6. Transmission T (a) and reflection spectra R (b) for LCP and RCP incidences and different values of b, the definition of which can be found in the inset of Figure 6a. The resultant circular dichroism for transmitted CD_T and reflected lights CD_R are shown in (c) and (d), respectively. Blue solid lines, green dashed, and red dotted ones represent the results for $b = 640$ nm, 720 nm, and 800 nm, respectively. The other structural and material parameters are the same as in Figure 6.

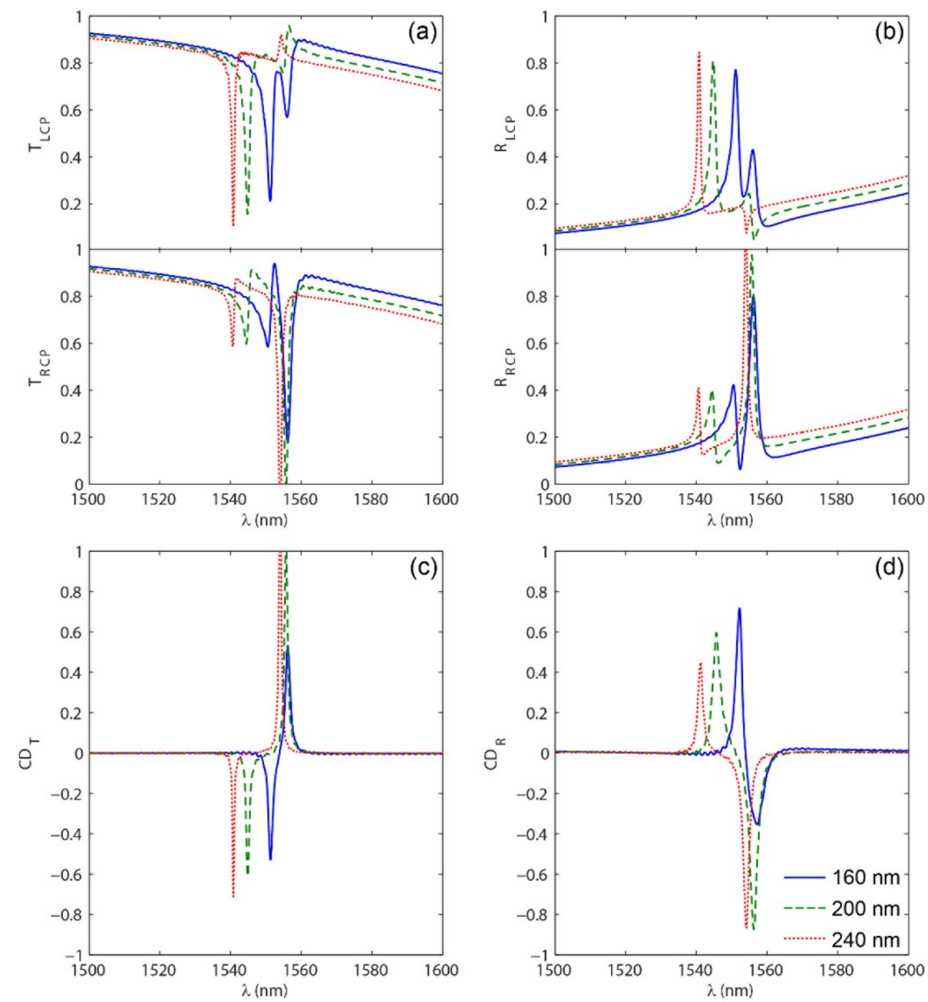

Figure S7. Transmission T (a) and reflection spectra R (b) for LCP and RCP incidences and different values of w, the definition of which can be found in the inset of Figure 6a. The resultant circular dichroism for transmitted CD_T and reflected lights CD_R are shown in (c) and (d), respectively. Blue solid lines, green dashed, and red dotted ones represent the results for $w = 160$ nm, 200 nm, and 240 nm, respectively. The other structural and material parameters are the same as in Figure 6.

References

[S1] V. A. Zenin, A. B. Evlyukhin, S. M. Novikov, Y. Yang, R. Malureanu, A. V. Lavrinenko, B. N. Chichkov, S. I. Bozhevolnyi, Direct Amplitude-Phase Near-Field Observation of Higher-Order Anapole States. *Nano Lett.* **2017**, 17, 7152-7159.